KSTLE International Journal, Vol. 4, No. 2, December 2003, pp. 60-66

Frictional Instabilities of Polymer Composite Containing Barite or Potassium Titanate for Brake Linings

Seong Jin Kim and Ho Jang†

Department of Advanced Materials Engineering, Korea University, 5-1, Anam-dong, Seongbuk-gu, Seoul 136-701, Korea

Abstract: Tribological properties of novolac resin composites containing particulate barite ($BaSO_4$) or potassium titanate ($K_2O \cdot 6(TiO_2)$) whiskers (two typical space fillers for commercial automotive brake linings) were investigated. The emphasis of the current investigation was given to the effect of the two fillers on the propensity of the stick-slip phenomena and formation of stable rubbing surface. A block-on-disk type tribometer was used for friction assessment. Results showed that the $BaSO_4$-filled composite produced large friction force oscillations at slow sliding speeds and created severe damage on the gray iron counter surface. On the other hand, the composite with $K_2O \cdot 6(TiO_2)$ whiskers formed a stable rubbing surface and showed smooth sliding behavior without large friction force fluctuation. The microscopic observation of the rubbing surface revealed that the $K_2O \cdot 6(TiO_2)$ whiskers played a key role in the formation of stable rubbing surface and smooth sliding behavior by effectively reinforcing the resin.

Keywords: Barite ($BaSO_4$), potassium titanate ($K_2O \cdot 6(TiO_2)$), filler, polymer composite, frictional oscillation, stick-slip

Introduction

The friction force oscillation during sliding is a very complicated phenomenon since it is dependent not only upon system dynamics but also on the material property of a friction couple. It is known that the oscillation during sliding is strongly affected by the stick-slip motion, which is an intermittent change of the friction force (or friction coefficient) [1,2]. Stick-slip occurs as a consequence of a combination of the system response, which is affected by damping, inertia, and stiffness of the system components, and its tribological properties at the sliding interface. It is widely accepted that the stick-slip occurs when the friction coefficient as a function of sliding speed shows a strong negative slope and/or when a difference ($\Delta\mu$) between the static (μ_s) and kinetic (μ_k) friction coefficient is large [3-5].

In the case of an automotive brake system, the stick-slip is produced by the tribological characteristics of a friction couple and the resultant intensity of the friction force oscillation is determined by the mechanical response of a system. Therefore, when brake induced noise and vibration occur during brake applications, the tribological property of a friction couple is urged to change to correct the problem and brake linings are usually modified first rather than changing gray iron rotors or drums. This is partly because the change of the lining formulation appears the convenient way to effectively modify tribological properties without changing major system design. In general, commercial brake linings contain more than 10 ingredients to satisfy safety and performance related requirements and designing a suitable brake lining comprises careful selections of raw material ingredients and demands many attempts to find an optimized formulation. A limited number of studies about brake-induced vibration and noise have been reported concerning the role of lining ingredients on the brake performance. Cho *et al.* [6] studied the role of raw material ingredients on the friction film formation and friction characteristics. They reported that the friction film formation on the gray iron disk is promoted by the solid lubricants and iron powders. They also reported that the friction film is not related to the coefficient of friction and fade resistance but reduces the amplitude of the friction force oscillation. Jang *et al.* [7] suggested that the friction material with a strong negative μ-v (friction coefficient vs. speed) relation exhibits stick-slip phenomena and tends to generate bigger torque variations (friction force oscillations) during brake applications. Brecht et al. [8] also showed that the difference between adhesion coefficient and dynamic friction coefficient is increased when the friction components are wet, resulting in high noise intensity. The effects of other ingredients such as abrasives, metals, lubricants, fibrous materials, binder resins, and friction modifiers on friction performance were also reported [9-14]. On the other hand, the studies about space fillers such as barite ($BaSO_4$) and potassium titanate ($K_2O \cdot 6(TiO_2)$) have not been reported although the quantity of the filler is much larger than any other ingredients. This is partly because they were assumed as inactive ingredients in determining the tribological characteristics.

In this work, friction characteristics of novolac resin composites containing particulate $BaSO_4$ and $K_2O \cdot 6(TiO_2)$ whiskers were investigated. We chose the two space fillers since they have been most frequently used for commercial

†Corresponding author; Tel: +82-2-3290-3276, Fax: +82-2-928-3584
E-mail: hojang@korea.ac.kr

Table 1. The composition and physical properties (average value) of the novolac resin composites investigated in this work

Specimen	Composition (vol.%)	Hardness (HRS)	Porosity (%)	Density (g/ml)
XR/BS	30% novolac resin+70% $BaSO_4$	121.6	6.69	3.22
XR/PT	30% novolac resin + 70% $K_2O \cdot 6(TiO_2)$	114.5	8.61	2.41

Table 2. The composition of the gray cast iron disk used for this study (wt.%). C.E. in this table indicates carbon equivalent: C.E. = $\%C + \%Si / 3$

C	Si	Mn	S	Cr	Cu	Mo	Ti	Nb	V	Fe	C.E.
3.35	2.35	0.66	0.11	0.28	0.22	0.025	0.048	0.003	0.01	Bal.	4.13

brake linings and they are different in morphology. In particular, we focused on the change of the tribological characteristics such as stick-slip, friction-induced oscillation, and morphology of rubbing surface according to the two different fillers. In this study, two component composite systems were employed to simplify the interpretation.

Experimental Details

Experimental specimens are resin-bonded friction composites containing two different fillers (Table 1). The resin used as a binder is a modified novolac type phenolic resin (Xylok, originally developed by Mid-land Silicones). $BaSO_4$ and $K_2O \cdot 6(TiO_2)$ are used as a filler for the composite material. Fig. 1 shows SEM micrographs of the two different fillers investigated in this work. The barite (#100, NBK) is fine granular particles with Mohs hardness 3-3.5 and specific gravity 4.5, while the potassium titanate (Tismo-D, Otsuka) is in the form of fine ceramic whiskers (needle shape) with $15 \pm 5\ \mu m$ in average length and $0.35 \pm 0.15\ \mu m$ in average diameter. The composites were manufactured by dry mixing, pre-forming, hot-pressing, and post-curing. Detailed manufacturing procedure and conditions for a friction composite can be found in previous publications [11,12]. The size of a composite for friction test is $12 \times 12 \times 5\ mm^3$. Worn surface morphology after friction tests was examined using a scanning electron microscope (Hitach S-4300). DMTA (dynamic mechanical thermal analysis) was performed to measure storage modulus of the composites using a dynamic mechanical analyzer (ARES, heating rate: 5°C/min, strain rate: 0.01%, and frequency: 0.5 Hz).

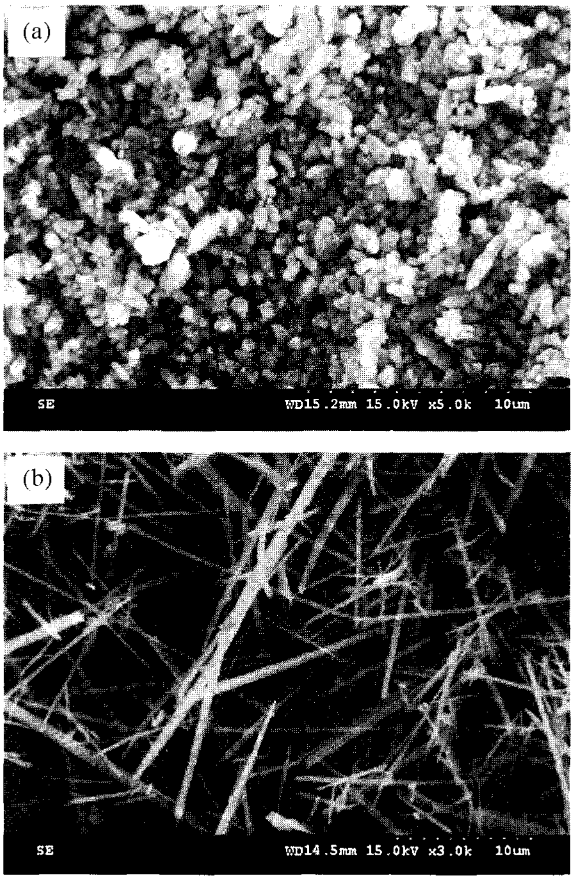

Fig. 1. SEM micrographs of two different fillers used in this work. (a) $BaSO_4$; (b) $K_2O \cdot 6(TiO_2)$.

The gray cast iron was used for counter disks and was 60 mm in diameter and 6 mm in thickness. The composition of the gray iron disk is given in Table 2. The microstructure of the disk showed A-type graphite flake with minimal B-type morphology (ASTM A247-67 designation) on a pearlite matrix. The surface hardness of the gray iron disk was in the range of $94.5 \pm 1.3\ HR_B$ (Rockwell hardness B scale). R_a (roughness average) of the disk surface before friction test was in the range of $0.08 \pm 0.01\ \mu m$. Disk surface was examined after friction tests using an optical microscope (Leica MZ6).

Friction tests were carried out using a block-on-disk type tribometer. A schematic diagram of the tribometer is shown in Fig. 2. The disk specimen is installed on a main spindle, which is driven by an AC servo motor (0.4 kW) connected to a magnetic coupling to isolate possible vibration from the motor unit. Normal force is applied using a dead weight and measured by a load cell. Friction tests were carried out at sliding velocity in the range of 1.57-47.1 mm/sec with the normal force of 15 N at room temperature. The specific torque (or friction force) at the sliding interface is measured by a torque sensor (TRT-50, Transducer Techniques Inc.). The output signals from the load cell and torque sensor are recorded by a PC-based data acquisition system (Lab-PC 1200, NI) at a sampling rate of 200 Hz. The disk run-out was carefully controlled at approximately $5\ \mu m$ for friction test. The run-out of the flat gray iron disk was measured by a non-contacting proximity sensor (Bently 3300 REBAM, $0.25\ \mu m$ resolution). The disk run-out was obtained from the peak-to-

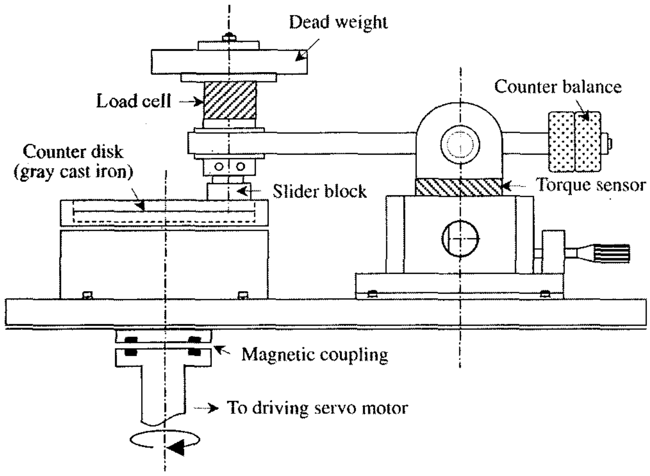

Fig. 2. A schematic diagram of the block-on-disk type tribometer used in this study.

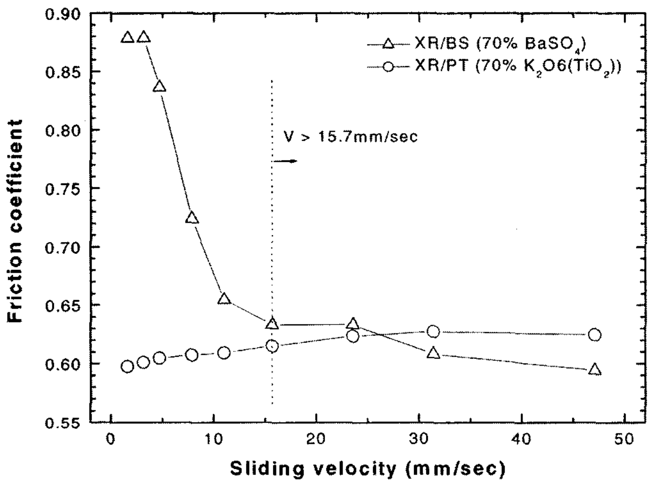

Fig. 3. The change of friction coefficient as a function of sliding velocity in the range of 1.57-47.1 mm/sec at 15 N of normal force.

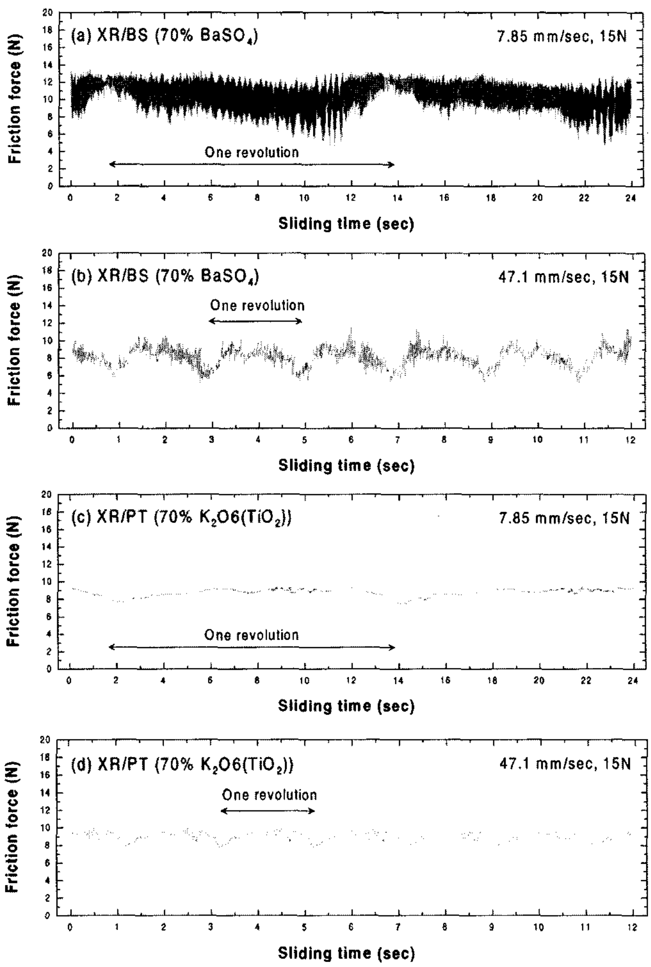

Fig. 4. The variation of friction force as a function of sliding time at two different sliding velocities: 7.85 and 47.1 mm/sec.

valley amplitude by measuring the distance between the probe and rotating disk surface.

Results and Discussion

The effect of sliding velocity on the coefficient of friction was investigated in the range of 1.57-47.1 mm/sec. Fig. 3 shows the change of friction coefficient as a function of sliding velocity for the composites containing two different fillers ($BaSO_4$ and $K_2O \cdot 6(TiO_2)$). At high velocities (>15.7 mm/sec) both composites showed similar coefficients of friction regardless of sliding velocities. On the other hand, the friction coefficient increased significantly at low velocities (<15.7 mm/sec) when $BaSO_4$ was used as a filler, indicating that the static coefficient of friction of $BaSO_4$ is much higher than the dynamic coefficient of friction. This is an important finding because the ingredient showing high speed sensitivity tends to accompany stick-slip during sliding and often degrade the brake performance [3,7]. In addition, this is contrary to the fact that the space fillers such as $BaSO_4$ and $K_2O \cdot 6(TiO_2)$ are considered as inert materials to various sliding conditions.

The amplitude of the friction force was measured to correlate the μ-v relation to the amplitude of friction-induced oscillation since the composite with large $\Delta\mu$ ($=\mu_s - \mu_k$) exhibits large force oscillations [7]. The run-out of the rotating disk was precisely controlled since the friction force oscillation can be affected by the amount of disk run-out. The initial run-out was set at 5.0 ± 0.2 μm in this experiment. Fig. 4(a)/(b) and (c)/(d) show the change of friction force at two different sliding velocities (7.85 and 47.1 mm/sec) for the $BaSO_4$ and $K_2O \cdot 6(TiO_2)$-filled composites. Two aspects of friction force oscillation are noteworthy in the Fig. 4. One is the difference in the intensity of the friction force oscillation per revolution and the other is the local variation of friction force within one revolution. Concerning the intensity of the friction force oscillation, the $BaSO_4$-filled composite (XR/BS) showed bigger fluctuation of friction force than the composite with $K_2O \cdot 6(TiO_2)$ at low sliding velocity ($v = 7.85$ mm/sec). The bigger oscillation in this case (Fig. 4(a)) appears due to the large $\Delta\mu$, combined with the slightly higher level of friction force in the case of the composite with $BaSO_4$. Another interesting observation was the amplitude of local friction

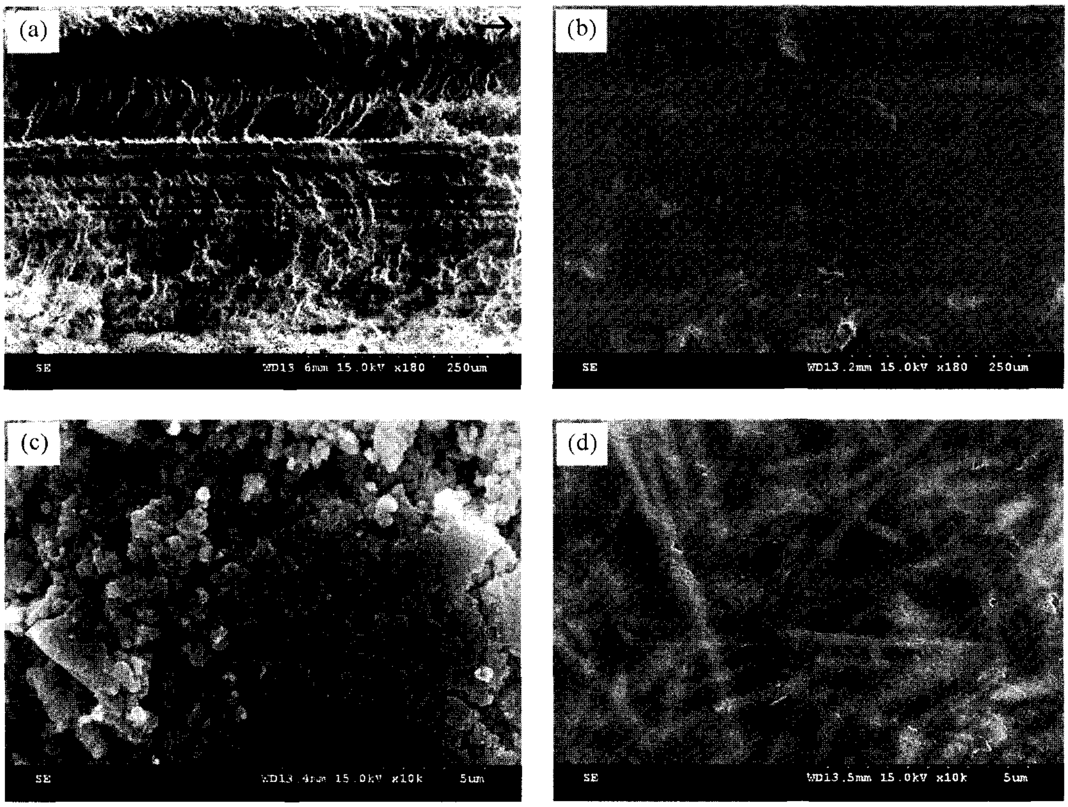

Fig. 5. SEM micrographs of worn surfaces of the two composites after friction tests. The micrographs were shown in two different magnifications ((180 and (10k). (a)/(c) $BaSO_4$-filled composite (XR/BS); (b)/(d) $K_2O \cdot 6(TiO_2)$-filled composite (XR/PT). The arrows indicate the sliding direction.

force variation within one revolution. Comparing Fig. 4(a) and (b), the amplitude of the averaged friction force variation is similar while the amount of friction force oscillation is much bigger at slow sliding speed suggesting that the friction force oscillation is affected by the level of average friction force and the stick-slip of the $BaSO_4$-filled composite. On the other hand, the composite with $K_2O \cdot 6(TiO_2)$ (XR/PT) showed a stable friction force regardless of sliding velocity.

In order to understand the difference in the sliding behavior of the two composites, morphology of the rubbing surface was examined using an SEM (Fig. 5). The figure shows that the rubbing surfaces of the composites after sliding experiments are significantly different. The rubbing surface of the composite with $BaSO_4$ showed a number of hair cracks in the direction perpendicular to the sliding direction with significant surface damage. The hair crack formation and the subsequent removal of the surface layer are attributed to the shear deformation of the material and they are normally associated with the production of large wear debris. On the other hand, the composite with $K_2O \cdot 6(TiO_2)$ showed a smooth and glossy surface with few hair cracks. The rubbing surfaces were also examined at a high magnification to examine the effect of the filler shape on the rubbing surface and to understand consequent tribological behaviors (Fig. 5(c) and (d)). They clearly indicated that the whisker shaped filler effectively reinforcing the matrix resin providing higher mechanical strength of the whisker-matrix interface than the particular

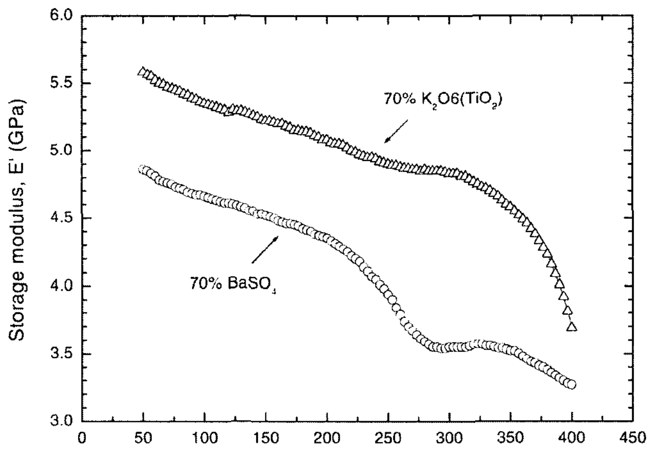

Fig. 6. Storage modulus (E') as a function of temperature for the novolac resin composites containing two different fillers.

shaped filler. The stable adherent rubbing surface, therefore, appears to be related with the smooth frictional behavior of the $K_2O \cdot 6(TiO_2)$-filled composite. On the other hand, the rubbed surface of XR/BS composite exhibited granular particles compacted during sliding, which is responsible for the hair crack formation and poor wear resistance of the $BaSO_4$-filled composite.

The surface morphology provides important information

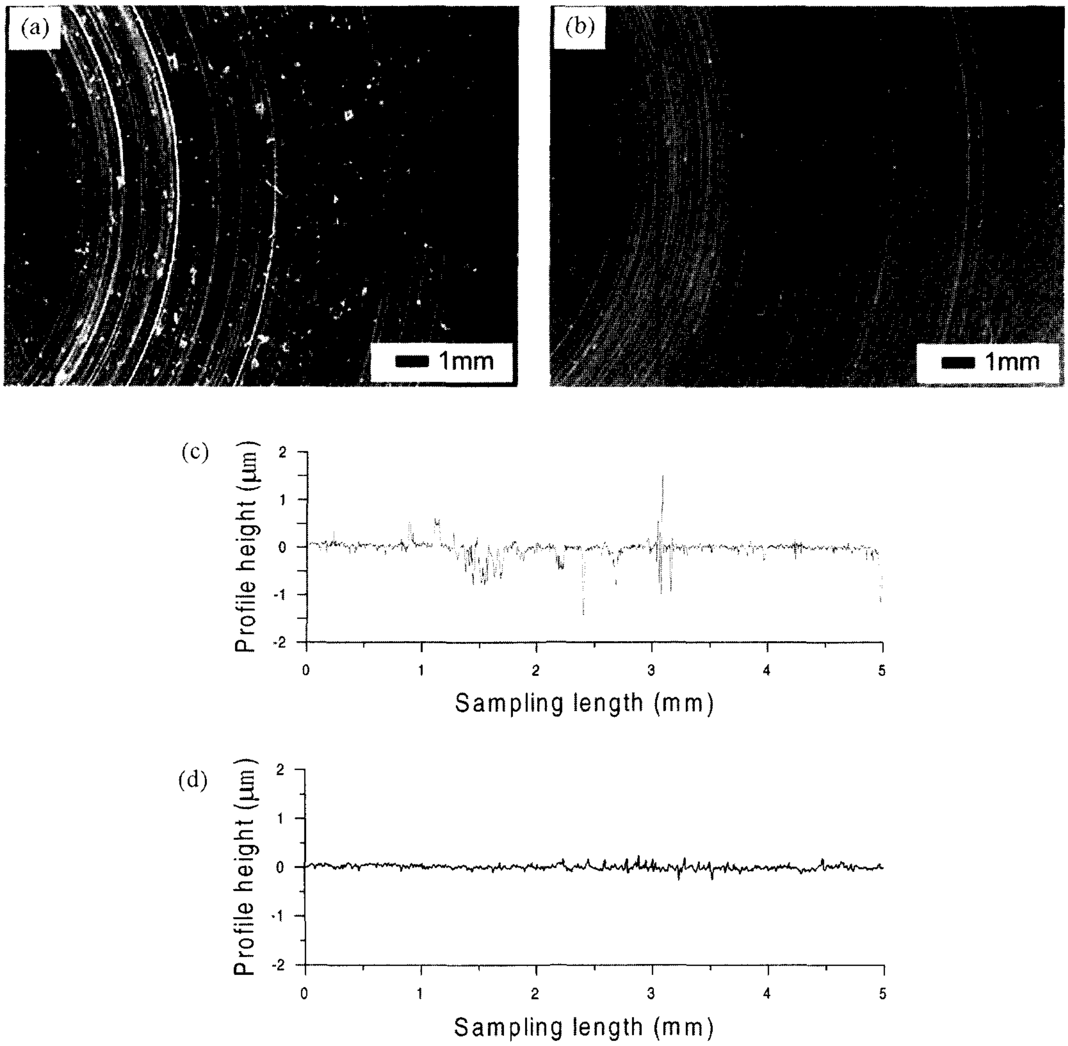

Fig. 7. Disc surface morphologies and surface profiles when the friction tests were performed with (a)/(c) $BaSO_4$-filled composite and (b)/(d) $K_2O \cdot 6(TiO_2)$-filled composite.

about the cause of friction force oscillation. This is because the stick-slip can be determined by the surface roughness and stiffness of the composite since the stiffness of the composite is known as an important factor to prevent the "irregular" stick-slip phenomena [3]. Therefore, the large friction force oscillation of the $BaSO_4$-filled composite appears due to the low stiffness of the composite combined with the large $\Delta\mu$. Mechanical strength of the composites was measured using DMTA to compare the stiffness of the two composites. Fig. 6 shows the storage modulus of the two composites, which is proportional to the stiffness of the composite. The figure shows that the storage modulus of the $K_2O \cdot 6(TiO_2)$-filled composite is higher than that of $BaSO_4$-filled composite at the temperature below 400°C due to effective reinforcement of $K_2O \cdot 6(TiO_2)$ whiskers, suggesting that the former composite is better in preventing the irregular stick-slip.

Wear tests were also performed to investigate the aggressiveness of $BaSO_4$ or $K_2O \cdot 6(TiO_2)$-filled composites against a gray iron counter disk. Fig. 7 shows the disk surface morphology and surface profile after friction tests (load: 15 N; sliding velocity: 1.57 mm/sec; sliding distance: 100 m). The figure indicates that the $BaSO_4$-filled composite damaged the disk surface more than $K_2O \cdot 6(TiO_2)$-filled composite, resulting in the increase of surface roughness. The figure also suggests that the particulate $BaSO_4$ is more aggressive than $K_2O \cdot 6(TiO_2)$ whiskers since the $BaSO_4$ particles are easily removed from the matrix and underwent rolling and scratching at the sliding interface.

Conclusions

Tribological properties of novolac resin composites filled with particulate $BaSO_4$ or $K_2O{\cdot}6(TiO_2)$ whiskers were investigated. The conclusions from this work are summarized as follows:

1. The composite containing $K_2O{\cdot}6(TiO_2)$ whiskers showed smaller amplitudes of friction force oscillation during sliding than the composite with $BaSO_4$.
2. The $BaSO_4$-filled composite showed a steep negative μ-v slope at lower sliding velocities (< 15.7 mm/sec). This indicates the large difference in the static and dynamic

coefficients of friction, causing "regular" stick-slip.

3. The large fluctuation of friction force oscillation was also due to the rough surface from insufficient reinforcement and low stiffness of the $BaSO_4$-filled composite by particulate $BaSO_4$, which is a cause of "irregular" stick-slip.
4. Friction force oscillation during sliding was closely associated with the stiffness of the composite, morphology of the rubbing surface, and the difference between static and dynamic coefficients of friction.

Acknowledgments

This work was supported by Korea University Post-Doc. Grant in the year 2003.

References

1. F.P. Bowden and D. Tabor, The Friction and Lubrication of Solids, Oxford Univ. Press, London, 1964.
2. B. Bhushan, Principles and Applications of Tribology, John Wiley & Sons, New York, 1999.
3. E. Rabinowicz, Friction and Wear of Materials, John Wiley & Sons, New York, 1995.
4. C. Gao and D. Kuhlmann-Wilsdorf, On Stick-Slip and the Velocity Dependence of Friction at Low Speeds, Trans. ASME J. Tribo., Vol. 112, pp. 354-360, 1990.
5. B. Feeny, A. Guran, N. Hinrichs and K. Popp, A Historical Review on Dry Friction and Stick-Slip Phenomena, Appl. Mech. Rev., Vol. 51, pp. 321-341, 1998.
6. M.H. Cho, E.G. Bae, H. Jang, G. Jeong, D. Kim and C. Choi, The Role of Raw Material Ingredients of Brake Linings on the Formation of Transfer Film and Friction Characteristics, SAE Tech. Paper, 2001-01-3130, pp. 49-54, 2001.
7. H. Jang, J.S. Lee and J.W. Fash, Compositional Effects of the Brake Friction Material on Creep Groan Phenomena, Wear, Vol.251, pp.1477-1483, 2001.
8. J. Brecht, W. Hoffricchter and A. Dohle, Mechanisms of Brake Creep Groan, SAE Tech. Paper, 973026, pp. 79-85, 1997.
9. H. Jang and S.J. Kim, The Effect of Antimony Trisulfide (Sb_2S_3) and Zirconium Silicate ($ZrSiO_4$) in the Automotive Brake Friction Material on Friction Characteristics, Wear, Vol. 239, pp. 229-236, 2000.
10. H. Jang, J.J. Lee, S.J. Kim and K.Y. Jung, The Effect of Solid Lubricants on Friction Characteristics, SAE Tech. Paper, 982235, pp. 1-8, 1998.
11. S.J. Kim, M.H. Cho, D.-S. Lim and H. Jang, Synergistic Effects of Aramid Pulp and Potassium Titanate Whiskers in the Automotive Friction Material, Wear, Vol. 251, pp. 1484-1491, 2001.
12. S.J. Kim, K.S. Kim and H. Jang, Optimization of Manufacturing Parameters for a Brake Lining Using Taguchi Method, J. Mater. Process. Tech., Vol. 136, pp. 202-208, 2003.
13. S.J. Kim and H. Jang, Friction and Wear of Friction Materials Containing Two Different Phenolic Resins Reinforced with Aramid Pulp, Tribo. Int., Vol. 33, pp. 477-484, 2000.
14. Y. Handa and T. Kato, Effects of Cu Powder, $BaSO_4$ and Cashew Dust on the Wear and Friction Characteristics of Automotive Brake Pads, Tribo. Trans., Vol. 39, pp. 346-353, 1996.